Journal of Mathematics and Statistics Studies
ISSN: 2709-4200
DOI: 10.32996/jmss
Journal Homepage: www.al-kindipublisher.com/index.php/jmss

JMSS
AL-KINDI CENTER FOR RESEARCH AND DEVELOPMENT

| RESEARCH ARTICLE

Thermal Transport of Forchheimer Nanofluid Flow with Permeable Medium and Optimal Internal Heat Source/Sink

Uka Uchenna. Awucha[1] ✉ Kanu Richmond. Uchenna[2], Amadi Okechukwu[3], Akindadelo Adedeji Tomide[4] and Bamisile, Oludare Olabode[5]

[1245]Department of Basic Sciences, School of Science and Technology, Babcock University, PMB 4003, Ilishan-Remo, Nigeria.
[3]Department of Mathematics, Ignatius Ajuru University of Education, Rumuolumeni, Port-Harcourt, Nigeria.
Corresponding Author: Uka Uchenna. Awucha, **E-mail**: ukau@babcock.edu.ng

| ABSTRACT

This study x-rays the analysis of convection heat transport of hydromagnetic Forchheimer nanofluid flow in the presence of an ideal internal heat source/sink. A similarity tactic is followed by translating the partial differential models into coupled nonlinear ordinary differential equations. The application of the improved series scheme made it possible for the solution to the translated problems to be found. Pictorial developments such as graphs with legends have been gotten by adopting the Wolfram Mathematica package for the sake of understanding the behavioral pattern of flow, temperature, and specie (nanoparticle) concentrations due to the influence of fluid parameters on them. Results demonstrated that an increase in flow and temperature occurs as buoyancy effect, and optimal heat generation number rises. Intensification of Prandtl number leads to a drop in the flow rate and temperature just as the concentration distribution declines for $s_n > 0$. The impact of fluid parameters on skin friction was also considered.

| KEYWORDS

Heat generation/absorption, Forchheimer Nanoliquid, Porous medium, Natural Convection, Series approach, Hydromagnetic.

| ARTICLE INFORMATION

ACCEPTED: 01 October 2022 **PUBLISHED:** 03 October 2022 **DOI:** 10.32996/jmss.2022.3.2.2

1. Introduction

Adequate heat transmission and controlling processes are paramount for optimal functioning and lifespan extension of industrial machines, electrical circuits, solar power collectors, etc. Therefore, in order to achieve a high degree of industrial machine efficiency, the conductivity of heat in a fluid through a medium is required to be at a normal rate. However, the thermal transfer rate is a function of the type of fluid being employed. Therefore, in order to achieve remarkable heat transmission through a medium, a fluid with high conductivity capacity becomes paramount. Hence, the need for nanofluid arises. In clear terms, nanofluid is made up of convectional fluids example, liquids, oils, ethylene glycol (ECG), etc., and particles in the form of oxides of metals, ceramics with high conductivity and chemical properties, as well as nanotubes and some sorts of carbon. Thus, in order to maintain stability and reduce the surface tension of the blend, the surfactant is sometimes added. The applications of this study range from the production of synthetic rubber sheets and plastic, drawing of cables and fiber sheets, production of papers, glass fiber production (blowing and spinning), spinning of steel, aluminum alloy, metals, cooling of an infinite hot metal sheet in a tub, an effective cooling process in the reactors of nuclear fission through the aid of electromagnetic forces in supplying liquified sodium to the nuclear power reactors through a process termed nuclear reactor fluidization. Similarly, the applications of this research in the aerospace and automotive, medical field, electronics, food manufacturing, and processing establishments are also of great importance. An input in quasi malleable fluid because of special features of being viscid as well as perfect polymer fluids are attributed to Willamson [1929]. Rasool and Wakif [2021] used spectral techniques to inquire about convection thermal transmission for the electro-magnetohydrodynamic second form fluid movement containing species (nanoparticles) by deploying Buongiorno's

posture for examination. Similarly, Benos et al. [2019] adopted the application of blood reliance on nanofluids in different medical pertinence. The aids due to nanofluid movement with diverse settings have been presented by Kumar et al. [2020]. Several natural phenomena appear in indirect order, whereas others are extremely direct in occurrence. In such cases, it becomes difficult to obtain their closed-form solutions. As a result of this, several scholars consider numerical or semi-analytical methodology. Nasir et al. [2018] applied the homotopy analysis method to resolve the problems. The study of chemical reaction and radiation effects on magnetohydrodynamic Nanofluid flow over a sheet stretching exponentially was reported by Uka et al. [2022]. Pal et al. [2010] reported the effect of heat radiation in flows that violates Darcy's law by becoming laminar in assembling, increasing more than the Reynolds parameter leading to a stormy form of flow. The non-linearity models are changed to become ordinary differential equations without linearity in them by employing the similarity conversion idea; hence, the ideal homotopy analysis technique helps in the solution procedure. Similarly, Amos and Uka [2022] anchored the hydromagnetic nanofluid passage past an exponentially stretching plate with radiation and nonuniform heat generation/absorption. The Jeffery constituents exist as one of the fluids which does not obey Newton's law of viscosity by forecasting the delay as well as reduction outcomes in fluid flow problems. Its fluid equations are vital in biomedical sciences, oil basin procedures as well as chemical expertise, Shehzad et al., [2012], Turyilmaoglu [2014], Ellahi and Hussain [2015]. The results on Nusselt and Sherwood factors were presented graphically by Dehghan [2010]. Sheikholeslami et al. [2014] explored micropolar fluid passage in a conduit with chemical reaction by adopting the perturbation approach in terms of homotopy. They affirmed that under suction as well as blowing, Reynolds and Paclet parameters show a connection between Nusselt and Sherwood factors. The analysis of free and forced convection movement of Jeffrey fluid past a disposed expanding material in the presence of a two-stratification impact was recorded by Hayat et al. [2017]. They opined that due to an increased curvature number, the rate of flow, heat, and diffusion graphs rises far from the cylinder. Also, the effect of heat and mass parameters leads to a lessening of both temperature and diffusion. Sui et al. [2016] investigated heat and mass transport in the midst of Cattaneo-Christov dual-diffusion in higher Maxwell nanofluid over an elongating plate. The observations from their report showed that viscoelastic easing context structure provides support to envisage the reduction flow features. The analysis of Darcy-Forchheimer's theory for studying both free and forced flow of convection in the presence of different viscosity and radiation has been considered by Pal and Mondal [2012]. However, due to the importance and applicability of heat transport processes in technological development, more researchers have developed a greater interest in this field of study. Thus, the investigation of Darcy-Forchheimer's impacts on viscous transportation past an external plain is attributed to Ganesh et al. [2016]. Their result indicated an increase in temperature as a result of viscid debauchery impact. Hayat et al. [2016] studied the Darcy-Forchheimer flow with a degree of coldness/hotness reliant on thermal conduction and Cattaneo-Christov thermal fluidity relation. An examination of the effect of thermophoresis as well as viscid indulgence over a soaked absorbent surface on Darcy-Forchheimer transmission is attributed to Saddek [2006]. The homotopy analytical means was used to examine the three-dimensional movement of Carreau fluid in the presence of a magnetic field Ellahi et al. [2017].

Thus, in this study, we shall model the fluid flow problem under consideration by using appropriate mathematical equations and conditions at the boundary of the wall. Also, analytical solutions and their numerical simulations shall be obtained in order to examine the impact of fluid parameters on the flow geometry. The results obtained will be showcased graphically and discussed in detail.

2. Mathematical Expressions

Consider an incompressible electrically conducting hydromagnetic convective heat conveyance Darcy-Forchheimer nanofluid flow in two-dimensional axes with one in the direction of the sheet as x and the other being vertical is represented by y. The temperature and concentration far from the plate are smaller than the ones on the exterior of the sheet, which remains unvaried. The sketched representation of the flow, as well as models describing the continuity, rate of flow, heat, and specie (nanoparticle) concentration, are represented as follows:

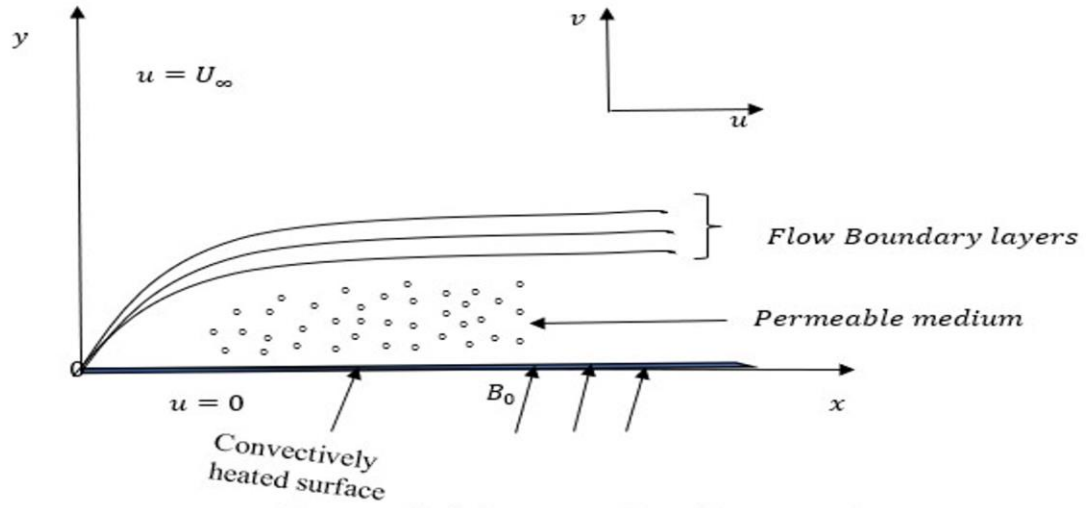

Figure a. Model representation with system of axes

$$\partial u/\partial x + \partial u/\partial y = 0 \quad (1)$$

$$u\,\partial u/\partial x + v\,\partial u/\partial y = \frac{\mu}{\rho}\partial^2 u/\partial y^2 - \sigma B_o^2/\rho\; u - 1/k_m\,(u^2 - u_\infty^2) + g\beta(T - T_\infty) + g\beta(C - C_\infty) \quad (2)$$

$$u\,\partial T/\partial x + v\,\partial T/\partial y = k/(\rho c)_f\,\partial^2 T/\partial y^2 + (\rho c)_p/(\rho c)_f\left[D_B(C - C_\infty)(T - T_\infty) + \frac{D_T}{T_\infty}(T - T_\infty)^2\right] + Q_h/\rho C_p\,(T - T_\infty) \quad (3)$$

$$u\;\partial C/\partial x + v\,\partial C/\partial y = D_m\,\partial^2 C/\partial y^2 + (\rho c)_p/(\rho c)_f\;D_T/T_\infty\,(T - T_\infty) \quad (4)$$

$$\begin{aligned} &u = 0, \quad v = s_v, \quad T = T_w, \quad C = C_\infty \quad \text{at } y = 0 \\ &u \to U_\infty, \quad T \to T_\infty, \quad C \to C_\infty \quad \text{as } y \to \infty \end{aligned} \quad (5)$$

Such that,

$\rho_f \Rightarrow$ density of fluid, $\sigma \Rightarrow$ electrical conduction number, $\beta \Rightarrow$ volumetric heat extension coefficient, $g \Rightarrow$ acceleration from gravity, $k \Rightarrow$ thermal transference, $\mu \Rightarrow$ fluid viscosity,

$D_T =$ thermophoresis diffusion coefficient, $D_B \Rightarrow$ Brownian movement quantity, temperature, T at the boundary, i.e., $y\ at\ zero \Rightarrow T_w$, ambient temperature $\Rightarrow T_\infty$, nanoparticle concentration $\Rightarrow C$, $\frac{\rho c_p}{\rho c_f} = \tau \Rightarrow$ ratio of heat capacity of specie nanoparticle to nanofluid, $Q_h \Rightarrow$ thermal factor.

The similarity transformation variables defined below shall be used.

$$\eta = y/\sqrt{\frac{u_\infty}{vx}}\,,\ \varphi = u_\infty\sqrt{vx/u_\infty}\,g(\eta)\,,\ \theta = T - T_\infty/T_w - T_\infty,\quad \emptyset = C - C_\infty/C_w - C_\infty$$

$$\begin{aligned} &T - T_\infty = \theta(\eta)(T_w - T_\infty), \quad T = \theta(\eta)(T_w - T_\infty) + T_\infty \\ &C - C_\infty = \emptyset(\eta)(C_w - C_\infty) \quad \Rightarrow \quad C = \emptyset(\eta)(C_w - C_\infty) + C_\infty \\ &v = -\partial\varphi/\partial x\,, u = \partial\varphi/\partial y \end{aligned} \quad (6)$$

From equation (1)

$\partial u/\partial x + \partial u/\partial y = 0$

Substituting $v = -\partial\varphi/\partial x\,, u = \partial\varphi/\partial y$ into equation (1) imply

$\partial^2\varphi/\partial x\partial y - \partial^2\varphi/\partial x\partial y = 0$

Thus, equation (1) holds.

Transforming equations (2) – (4) using equation (6) and simplifying further yields,

$$\partial^3 g/\partial\eta^3 + 1/2\,g\,\partial^2 g/\partial\eta^2 + \beta\left(1 - \left(\partial g/\partial\eta\right)^2\right) - H\,\partial g/\partial\eta + G_t f(\eta) + G_s\emptyset(\eta) = 0 \quad (7)$$

$$\partial^2 f/\partial\eta^2 + Prf(\eta)\,\partial f/\partial\eta + B_m f(\eta)\emptyset(\eta) + T_P f(\eta) + Qf(\eta) = 0 \quad (8)$$

$$\partial^2 \emptyset/\partial\eta^2 + Scf(\eta)\,\partial\emptyset/\partial\eta + {T_P}/{B_m}\, f(\eta) = 0 \quad (9)$$

In line with $g'(0) = 1,\ g(0) = Z_0,\ f(0) = 1,\ \emptyset(0) = 1$, for $\eta = 0$

$$g'(\infty) \to 0,\ f(\infty) \to 0,\ \emptyset(\infty) \to 0, \ni \eta \to \infty \quad (10)$$

with,

$$\beta = {1}/{K_m}\, x, H = {\sigma B_0^2 x}/{\rho U_\infty}, G_t = {\beta g f(T_w - T_\infty)x}/{U_\infty^2}, G_s = {\beta g \emptyset(C_w - C_\infty)x}/{U_\infty^2}, Pr = {\vartheta}/{\alpha},$$

$$M_B = {\alpha D_B(C_w - C_\infty)x}/{U_\infty^2}, T_P = {\mu D_{T(C_w - C_\infty)x}}/{\nu T_\infty}, Sc = {v}/{D_m}, g_0 = {Z_w}\Big/{y/\sqrt{\frac{vx}{U_\infty}}}$$

refers to permeability, Hartmann, modified heat and mass Grashof, Prandtl, Brownian motion, Thermophoresis, Schmidt, and Suction numbers accordingly.

3. Methods and Solution Setup

Let

$$\eta = \Gamma g_0,\ g(\eta) = g_0 G(\eta),\ f(\eta) = h(\eta),\ \emptyset(\eta) = z(\eta),\ \varrho = {1}/{g_o^2} \quad (11)$$

Using equation (11) in equation (7) – (9), will yield

$$\partial^3 G/\partial\eta^3 + {1}/{2}\, G\,\partial^2 G/\partial\eta^2 + \beta\varrho^2 - \beta\left(\partial G/\partial\eta\right)^2 - H\,\partial G/\partial\eta\,\varrho + G_t h(\eta)\varrho^2 + G_s z(\eta)\varrho^2 = 0 \quad (12)$$

$$\partial^2 h/\partial\eta^2 + PrG(\eta)\,\partial h/\partial\eta + B_m h(\eta)Z(\eta)\varrho + T_P h(\eta)\varrho + Qh(\eta)\varrho = 0 \quad (13)$$

$$\partial^2 z/\partial\eta^2 + ScG(\eta)\,\partial z/\partial\eta + {T_P}/{B_m}\, h(\eta)\varrho = 0 \quad (14)$$

With

$$G(0) = 1,\ G'(0) = \varrho,\ G'(\infty) = 0,\ h(0) = 1,\ h(\infty) = 0,\ Z(0) = 1,\ Z(\infty) = 0 \quad (15)$$

In the case of $\varrho \ll 1$, series approach becomes necessary by adopting the solutions as stated thus:

$$G(\eta) = 1 + \varrho G_1(\eta) + \varrho^2 G_2(\eta) + \cdots \quad (16)$$

$$h(\eta) = h_0(\eta) + \varrho h_1(\eta) + \cdots \quad (17)$$

$$Z(\eta) = Z_0(\eta) + \varrho Z_1(\eta) + \cdots \quad (18)$$

Differentiating equations (16) – (18) with respect to η, making the substitution of the results into equations (12) - (14), and considering the same index of corresponding coefficients will produce:

$$\partial^2 h_0/\partial\eta^2 + Pr\,\partial h_0/\partial\eta = 0;\ h_0(0) = 1, \quad h_0(\infty) = 0 \quad (19)$$

$$\partial^2 Z_0/\partial\eta^2 + Sc\,\partial Z_0/\partial\eta = 0;\ Z_0(0) = 1, \quad Z_0(\infty) = 0 \quad (20)$$

$$\partial^3 G_1/\partial\eta^3 + {1}/{2}\,\partial^2 G_1/\partial\eta^2 = 0; \quad G_1(0) = 0, \quad \partial G_1/\partial\eta\,(0) = 1, \quad \partial G_1/\partial\eta\,(\infty) = 0 \quad (21)$$

$$\partial^2 h_1/\partial\eta^2 + Pr\,\partial h_1/\partial\eta + PrG_1(\eta)\,\partial h_0/\partial\eta + B_m h_0(\eta)Z_0(\eta) + T_P h_0(\eta) + Qh_0(\eta) = 0 \quad (22)$$

$$h_1(0) = 0, \quad h_1(\infty) = 0$$

$$\partial^2 Z_1/\partial\eta^2 + Sc\,\partial Z_1/\partial\eta + ScG_1(\eta)\,\partial Z_0/\partial\eta + {T_P}/{B_m}\, h_0(\eta) = 0; \quad Z_1(0) = 0, \quad Z_1(\infty) = 0 \quad (23)$$

$$\partial^3 G_2/\partial\eta^3 + \tfrac{1}{2}\partial^2 G_2/\partial\eta^2 + {1}/{2}\, G_1\,\partial^2 G_1/\partial\eta^2 + \beta - \beta\left(\partial G_1/\partial\eta\right)^2 - H\,\partial G_1/\partial\eta + G_t h_0(\eta) + G_s Z_0(\eta) = 0$$

$$G_2(0) = 0, \quad \partial G_2/\partial\eta\,(0) = 1, \quad \partial G_2/\partial\eta\,(\infty) = 0 \quad (24)$$

Equations (19) – (24) are solved analytically for the velocity, temperature, and concentration and presented as follows:

$$g'(\eta) = exp - {1}/{2}\,\eta + \delta(-2\eta exp - {1}/{2}\,\eta + exp - {1}/{2}\,\eta - exp - \eta + 2\beta\eta - 4\beta + 2\beta exp - \eta - 4H\eta exp - {1}/{2}\,\eta + 4Hexp - {1}/{2}\,\eta - \frac{2\mathrm{Gt}}{\mathrm{Pr}(2\mathrm{Pr}-1)} exp - Pr\eta - \frac{2\mathrm{Gs}}{\mathrm{Sc}(2\mathrm{Sc}-1)} exp - Sc\eta - 4Hexp - {1}/{2}\,\eta - 4\beta\eta exp - {1}/{2}\,\eta + 2\beta exp - {1}/{2}\,\eta + \frac{2\mathrm{Gt}}{\mathrm{Pr}(2\mathrm{Pr}-1)} exp - {1}/{2}\,\eta + \frac{2\mathrm{Gs}}{\mathrm{Sc}(2\mathrm{Sc}-1)} exp - {1}/{2}\,\eta) \quad (25)$$

$$h(\eta) = exp - Pr\eta + \delta(2\eta exp - Pr\eta + {8\mathrm{Pr}}/{1 + 2\mathrm{Pr}}\, exp - \left({1}/{2} + Pr\right)\eta - {\mathrm{Nb}}/{\mathrm{Sc}(\mathrm{Pr} + \mathrm{Sc})}\, exp - (Sc + Pr)\eta + {\mathrm{Nt}}/{Pr}\,\eta exp - Pr\eta + {Q}/{\mathrm{Pr}}\,\eta exp - Pr\eta + {\mathrm{Nb}}/{\mathrm{Sc}(\mathrm{Pr} + \mathrm{Sc})}\, exp - Pr\eta - {8\mathrm{Pr}}/{1 + 2\mathrm{Pr}}\, exp - Pr\eta) \quad (26)$$

$$Z(\eta) = exp - Sc\eta + \delta(-2Sc\eta exp - Sc\eta - {}^{8(Sc)^2}/_{1+2Sc}\, exp - ({}^{1}/_{2} + Sc)\eta - {}^{Nt}/_{PrNb(Pr-Sc)}\, exp - Pr\eta + {}^{8(Sc)^2}/_{1+2Sc}\, exp - Sc\eta + {}^{Nt}/_{PrNb(Pr-Sc)}\, exp - Sc\eta) \quad (27)$$

Note: $\delta = 0.01$. The numerical simulation of equations (25) – (27) is enabled by the usage of Mathematica and Wolfran language. However, quantities of interest in the engineering development are stated as $g''(0) = g_o^3 G''$ for the skin friction due to the rate of flow,

$h'(0) = g_o h'$ refers to Nusselt factor associated with the rate of heat transportation coefficient, and the Sherwood factors regarding the concentration transmission coefficient imply

$z'(0) = g_o z'$. Thus, the following results in legend form seek to provide a clearer insight into this study.

4. Results and Discussion

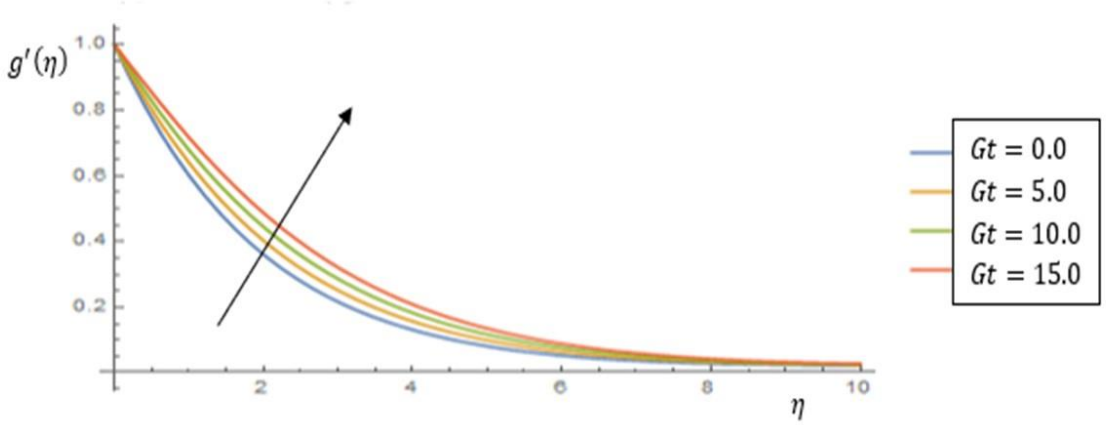

Figure 2. Influence of Modified heat Grashof factor, Gt on velocity at $\beta = 0.1, Gs = 2.0, Pr = 0.71, Sc = 1.0, H = 0.1$

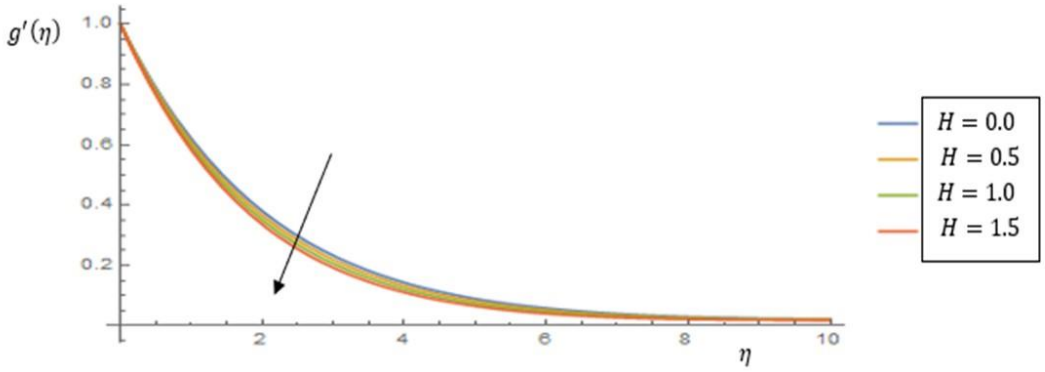

Figure 1. Influence of Hartmann number, H on velocity at $\beta = 0.1, Gt = Gs = 2.0, Pr = 0.71, Sc = 1.0$

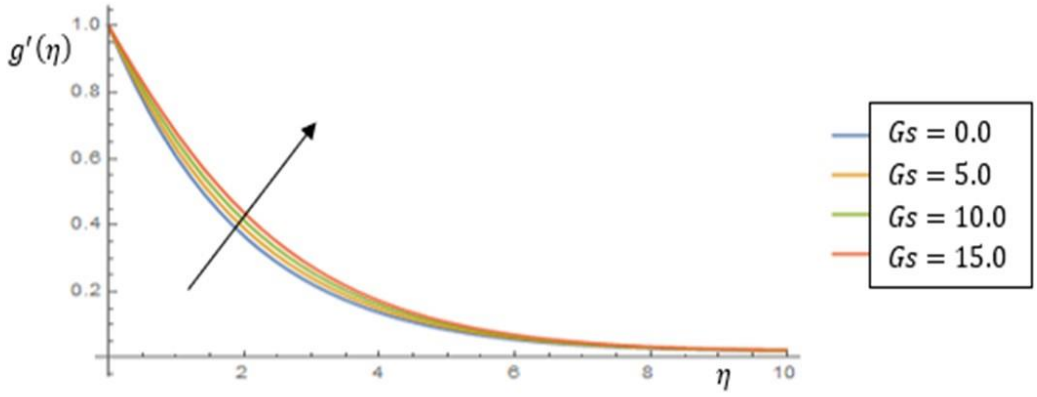

Figure 3. Influence of Modified mass Grashof factor, Gs on velocity at $\beta = 0.1, Gt = 2.0, Pr = 0.71, Sc = 1.0, H = 0.1$

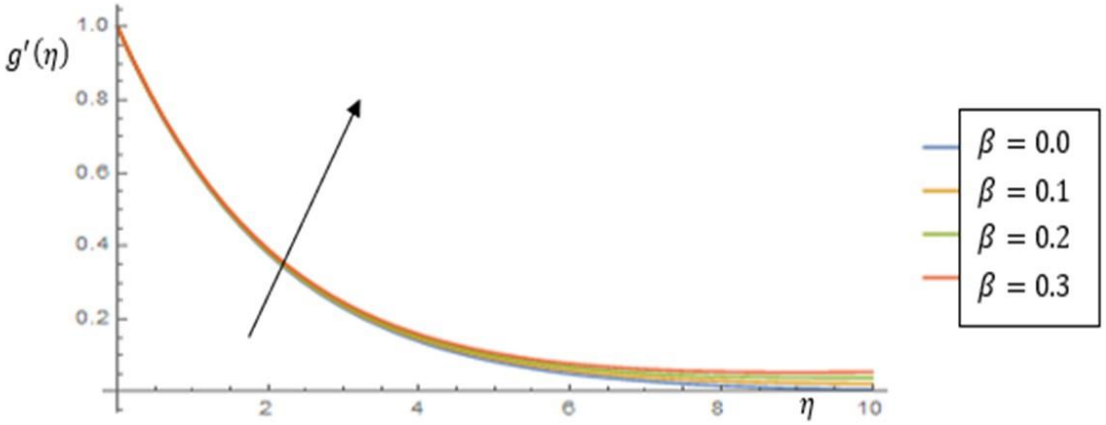

Figure 4. Influence of Permeability factor, β on velocity at $Gt = Gs = 2.0, Pr = 0.71, Sc = 1.0, H = 0.1$

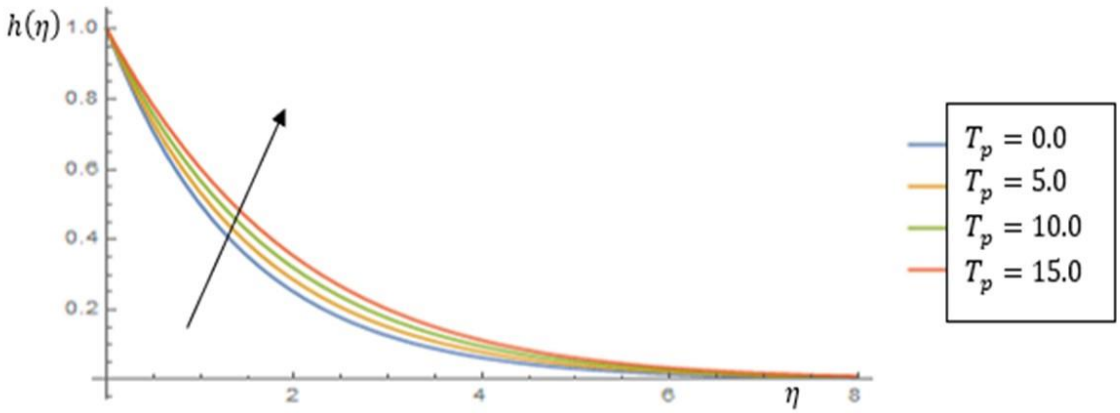

Figure 5. Influence of Thermophoresis factor, T_p on Temperature at $B_m = Q = 0.1, Pr = 0.71, Sc = 1.0$

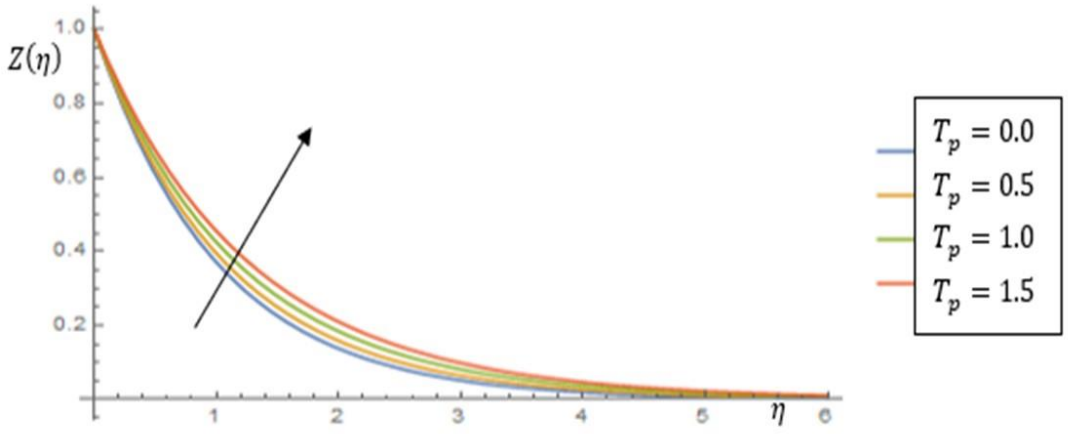

Figure 6. Influence of Thermophoresis factor, T_p on Concentration at $B_m = 0.1, Pr = 0.71, Sc = 1.0$

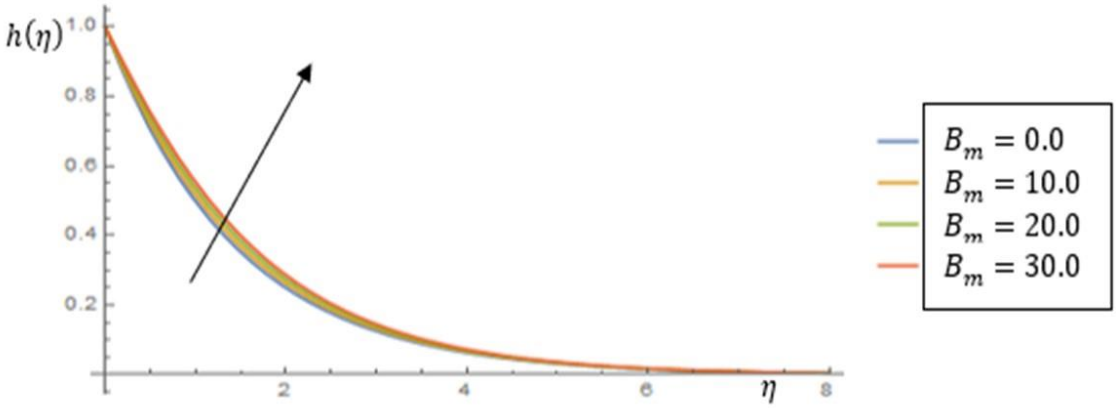

Figure 7. Influence of Brownian motion number, B_m on Temperature at $T_p = Q = 0.1, Pr = 0.71, Sc = 1.0$

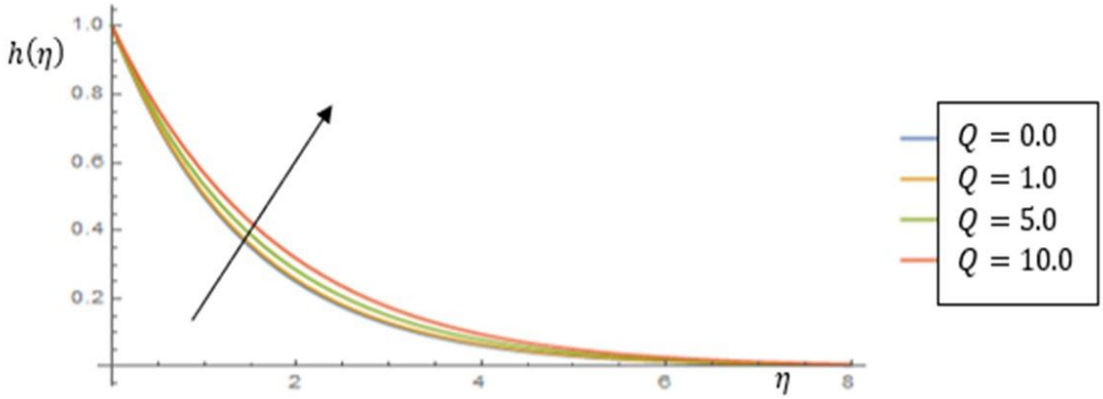

Figure 8. Influence of Heat generation number, $Q > 0$ on Temperature at $T_p = B_m = 0.1, Pr = 0.71, Sc = 1.0$

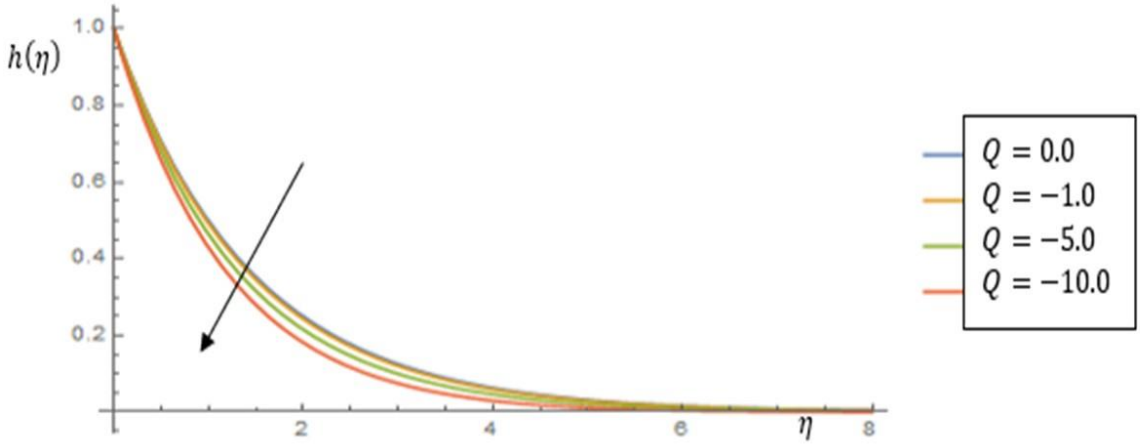

Figure 9. Influence of Heat absorption number, $Q < 0$ on Temperature at $T_p = B_m = 0.1, Pr = 0.71, Sc = 1.0$

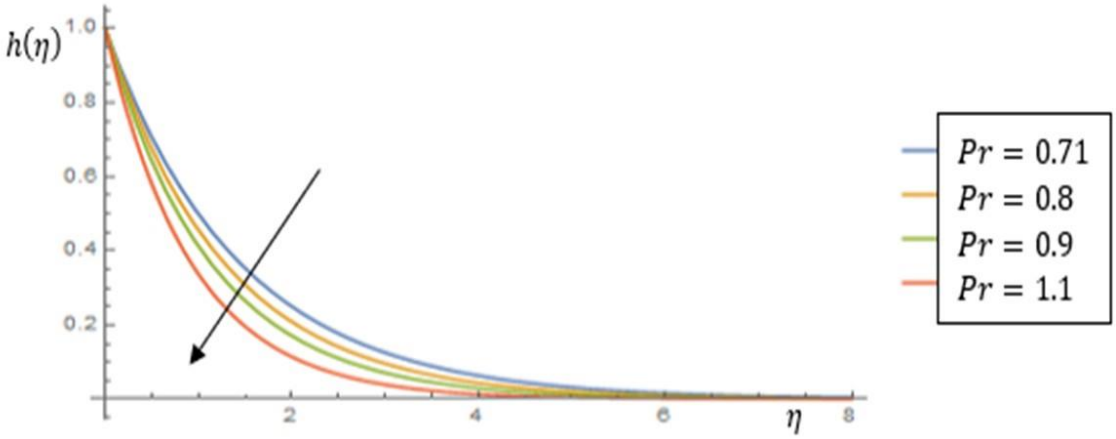

Figure 10. Influence of Prandtl parameter, Pr on Temperature at $T_p = B_m = Q = 0.1, Sc = 1.0$

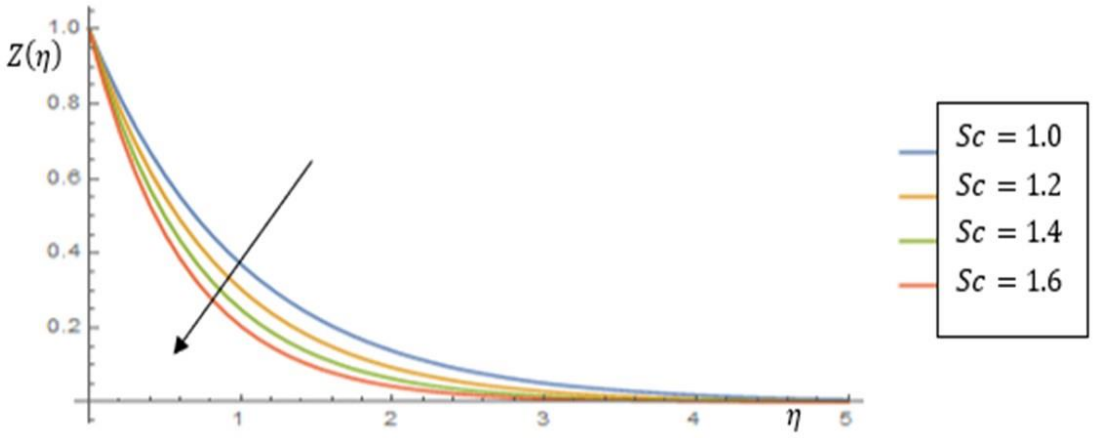

Figure 11. Influence of Schmidt number, Sc on Concentration at $B_m = T_p = 0.1, Pr = 0.71$

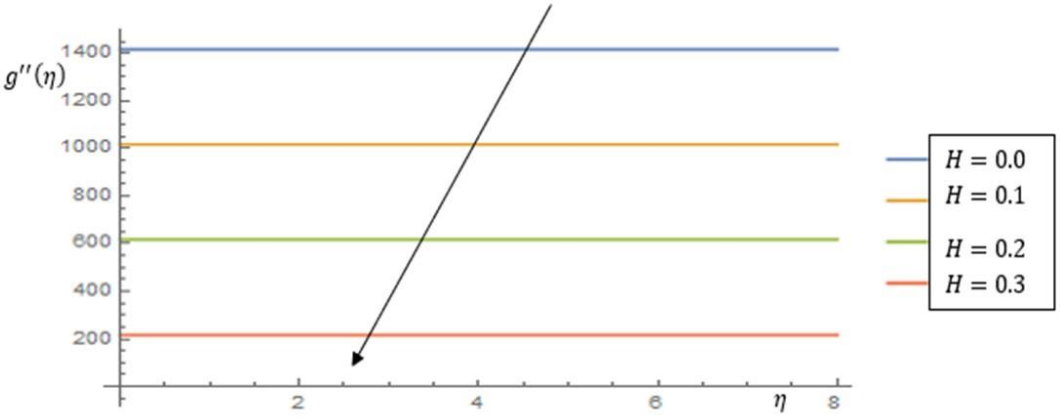

Figure 12. Influence of Hartman number, H on Skin friction at $\beta = 0.1, Gt = 2.0, Pr = 0.71, Sc = 1.0, Gs = 0.0$

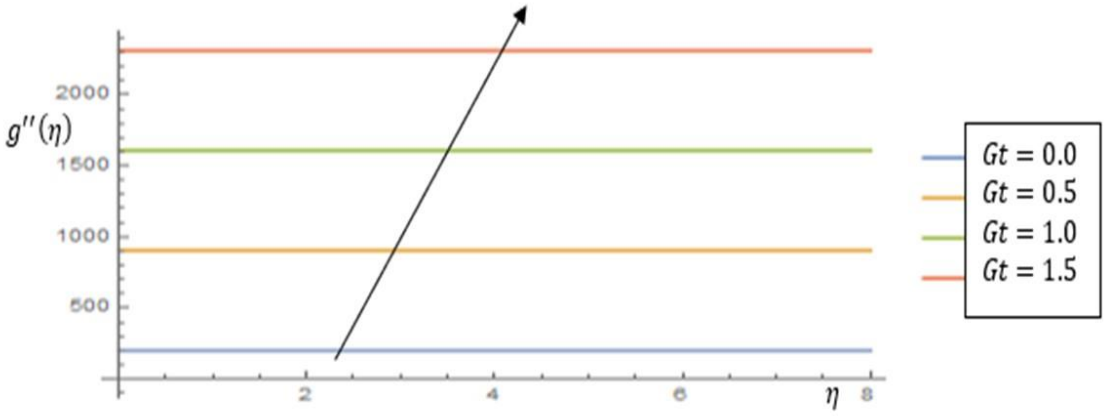

Figure 13. Influence of Thermal Grashof factor, Gt on Skin friction at $\beta = 0.1, Gs = 2.0, Pr = 0.71, Sc = 1.0, H = 0.1$

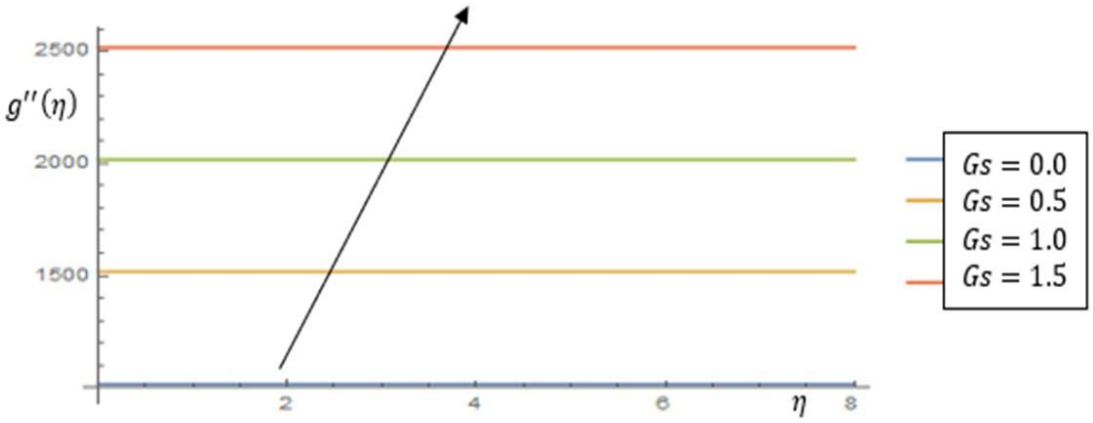

Figure 14. Influence of Concentration Grashof factor, Gt on Skin friction at $\beta = 0.1, Gt = 2.0, Pr = 0.71, Sc = 1.0, H = 0.1$

From the legends displayed above, the vertical axis stands for the dimensionless velocity, temperature, and nanoparticle concentration, while the horizontal axis shows the similarity variable. The effect of the fluid parameters on the various flow fields has been obtained as each of them is varied, just as the other remains unchanged.

The effect of the Hartman factor H on the velocity is captured in figure 1. It shows that velocity decreases as the parameter rises. Actually, impeding energy, referred to as Lorentz force, exists in the flow and forms a sort of resistance feature, hence the decrease in the rate of fluid flow. The evolution of modified heat Grashof parameter Gt is evidenced in figure 2. As convection intensifies in the fluid, more energy is gained, thus leading to an enhancement in the velocity. In figure 3, the impact of the modified mass Grashof factor on the velocity has been shown. The velocity surges as this number rises. The influence of the Forcchiemer

permeability variable β on the flow rate is highlighted in figure 4. When this viable parameter is raised, the more fluid passage will set in, thereby increasing the velocity of the fluid. Figures 5 and 6 depict the result of the thermophoresis factor on the temperature and concentration of the nanoparticles in the nanofluid. Really, this parameter relates to the difference in a temperature gradient, and as it intensifies, the heated surface conveys the heat to the cooler part, thereby heating it up while more heat energy is added to nanoparticle concentration which leads to an increase in their kinetic energy. Thus, the heat and mass boundary layers improve, leading to an increase in the temperature and concentration. The effect of the Brownian motion number on temperature is noticeable in figure 7. Due to the rise in the heat energy possessed by the nanoparticles as a result of their random motion, the thermal boundary layer becomes thinner as the temperature increases. The illustration of the outcome of the heat source and sink is shown in figures 8 and 9, respectively. Addition of heat ($Q > 0$) to the fluid leads to an enhancement of thermal energy and boundary layer. Thus, this brings about an intensification of temperature while the reverse will be the case, i.e., temperature decreases when there is the removal of heat ($Q < 0$) from the fluid. In figure 10, the effectiveness of the Prandtl parameter on temperature is presented. When this number is < 1, the thermal boundary layer becomes thicker but remains thinner as it is > 1.1. The Prandtl number is of great value in terms of its cooling characteristics in conducting fluids. Hence, increasing it amounts to a reduction in temperature. The effect of the Schmidt number on the concentration distribution is offered in figure 11. This number accounts for the ratio of the viscous diffusivity rate to that of mass diffusivity. When it is raised, there's a decrease in the boundary layer, and this causes a reduction in the concentration profile. However, intensification of Hartman, Permeability, thermal, and concentration Grashof factors depicts a rise in skin friction as noted in figures 12 – 15.

5. Conclusion

This current study investigates the analysis of hydromagnetic Convective heat Transport of Forchheimer nanofluid flow with a nonlinearly permeable surface and optimal internal heat source/sink through numerical means. Based on the findings from this work, the following conclusion follows:

(i) Enhancement of the permeability, modified heat, and concentration Grashof factors entail intensification of the velocity. (ii) An increase in the Hartman number leads to a decrease in the rate of fluid flow. (iii) A rise in the thermophoresis, Brownian motion, and heat generation ($Q > 0$) numbers are associated with an increase in temperature. (iv) A decreasing temperature distribution is evident in the case of heat absorption ($Q < 0$) and $Pr > 0$. (v) The concentration field rises as the thermophoresis number enhances, while it falls when the Schmidt number is intensified.
(vi) The distribution of the skin friction rises with the Hartman, Permeability, Thermal, and concentration Grashof factors.

5.1 Contribution to Knowledge

Based on the findings from this work, heat transfer serves as a vital concept in different industrial and engineering progressions. Thus, the relevance of this work cannot be overemphasized due to its application to civil, mechanical, and chemical engineering processes since heat transfer plays an important role in material selection, machinery efficiency, and reaction kinetics. Also, this study has revealed that the spray-drying technology depends on intensive heat transfer. However, spray-drying is a quick, continuous, cost-effective, reproducible, and scalable process for the production of dry powers from a fluid material by atomization through an atomizer into a hot drying gas medium such as air. In terms of technological advancement, this study has also showed that heat exchangers and mechanisms are highly useful in refrigeration, air conditioning systems, space heating, power generation, etc.; thus, a good example of a heat exchanger is the radiator in an automobile, i.e., car, in which the dual performing fluids refers to air and coolant. With the flowing of air around the radiator, heat is conveyed to the air from such coolant, and the essence of the air is to expunge heat from the coolant, thereby making the coolant depart from the radiator at a given lesser temperature level than it moves in.

5.2 Research limitations and Further Research

This study is limited to the steady case in two-dimensional forms. Also, it considers the Forchheimer Nanofluid. Thus, future research can be examined with consideration given to an unsteady case, three-dimensional components with non-Newtonian fluids.

Funding: This research received no external funding.
Conflicts of Interest: The authors declare no conflict of interest.
Acknowledgment: My appreciation goes to all my colleagues for their contributions to knowledge for a better world.

References

[1] Amos, E., & Uka, U. A. (n.d). Hydromagnetic Nanofluid Flow over an Exponentially Stretching Sheet in the Presence of Radiation and Nonuniform Heat Generation/Absorption.

[2] Benos, L., Spyrou, L. A., & Sarris, I. E. (2019). Development of a new theoretical model for blood-CNTs effective thermal conductivity pertaining to hyperthermia therapy of glioblastoma multiform. *Computer Methods and Programs in Biomedicine*, *172*, 79-85.

[3] Dehghan, M., Manafian, J., & Saadatmandi, A. (2010). Solving nonlinear fractional partial differential equations using the homotopy analysis method. *Numerical Methods for Partial Differential Equations: An International Journal*, *26*(2), 448-479.

[4] Ellahi, R., & Hussain, F. (2015). Simultaneous effects of MHD and partial slip on peristaltic flow of Jeffery fluid in a rectangular duct. *Journal of Magnetism and Magnetic Materials*, *393*, 284-292.

[5] Ellahi, R, Bhatti, M. M., Khalique, C. M.. (2017). 3D passage investigation of Carreaufluid model made by peristaltic wave with the magnetic field, *J Mol Liqs* 241 1059-1068.

[6] Ganesh, N. V. Hakeem, A. K. A. and Ganga, B. (2016). Darcy-Forchheimer passage of hydromagnetic nanofluid past a stretching plate under heated bedded media, second order slip, glutinous and Ohmic degeneracy impact, *Ain Shams Eng J* 9939-951.

[7] Kumar, K. G., Rahimi-Gorji, M., Reddy, M. G., Chamkha, A., & Alarifi, I. M. (2020). Enhancement of heat transfer in a convergent/divergent channel by using carbon nanotubes in the presence of a Darcy–Forchheimer medium. *Microsystem Technologies*, *26*(2), 323-332.

[8] Majeed, A., Zeeshan, A., & Noori, F. M. (2019). Numerical study of Darcy-Forchheimer model with activation energy subject to chemically reactive species and momentum slip of order two. *AIP Advances*, *9*(4), 045035.

[9] Nasir, S., Islam, S., Gul, T., Shah, Z., Khan, M. A., Khan, W., ... & Khan, S. (2018). Three-dimensional rotating flow of MHD single wall carbon nanotubes over a stretching sheet in the presence of thermal radiation. *Applied Nanoscience*, *8*(6), 1361-1378.

[10] Pasha, A. A., Rahman, M. M., Jamshed, W., Juhany, K. A., & Pillai, S. N. (2022). Buoyancy-driven flow and slippage constraints influences on Casson hybridity nanofluid of Yamada-Ota and Xue type via rotating cone. *Ain Shams Engineering Journal*, 101934.

[11] Pal, D and Chatterjee S. (2010). Heat and mass transport in MHD non-Darcian transmission with micropolar fluid past an extending plate immersed in a spongy medium involving non-similar heat generation and radiation, *Commun Nonlinear Sci Numer Simul* 15 1843-1857.

[12] Rasool, G., & Wakif, A. (2021). Numerical spectral examination of EMHD mixed convective flow of second-grade nanofluid towards a vertical Riga plate using an advanced version of the revised Buongiorno's nanofluid model. *Journal of Thermal Analysis and Calorimetry*, *143*(3), 2379-2393.

[13] Shehzad, S. A., Alsaedi, A., & Hayat, T. (2012). The three-dimensional flow of Jeffery fluid with convective surface boundary conditions. *International Journal of Heat and Mass Transfer*, *55*(15-16), 3971-3976.

[14] Sheikholeslami, M., Hatami, M., & Ganji, D. D. (2014). Micropolar fluid flow and heat transfer in a permeable channel using analytical method. *Journal of Molecular Liquids*, *194*, 30-36.

[15] Sui, J., Zheng, L and Zhang, X. (2016).Boundary stratification thermal and mass transport in the presence of Cattaneo-Christov dual-diffusion in upper-convectively Maxwell nanofluid over an elastic sheet and slip velocity, *Int J Thermal Sci* 194 461-468.

[16] Seddek, M. A. (2006). Effect of sticky dissipation, thermophoresis on Darcy-Forchheimer free and forced convective fluid wet leaky medium, *J Colloid and Interface S* 293 (2006)137-142.

[17] Turkyilmazoglu, M. (2014). Extending the traditional Jeffery-Hamel flow to stretchable convergent/divergent channels. *Computers & Fluids*, *100*, 196-203.

[18] Ur Rasheed, H., AL-Zubaidi, A., Islam, S., Saleem, S., Khan, Z., & Khan, W. (2021). Effects of Joule heating and viscous dissipation on magnetohydrodynamic boundary layer flow of Jeffrey nanofluid over a vertically stretching cylinder. *Coatings*, *11*(3), 353.

[19] Uka, U. A., Amos, E., & Nwaigwe, C. Chemical Reaction and Thermal Radiation Effects on Magnetohydrodynamic Nanofluid Flow Past an Exponentially Stretching Sheet.

[20] Williamson, R. (1929). The flow of pseudoplastic materials. *Industrial & Engineering Chemistry* 21, no: 1108-1111.